

Effective Connectivity in Depression

Edmund T. Rolls, Wei Cheng, Matthieu Gilson, Jiang Qiu, Zicheng Hu, Hongtao Ruan, Yu Li, Chu-Chung Huang, Albert C. Yang, Shih-Jen Tsai, Xiaodong Zhang, Kaixiang Zhuang, Ching-Po Lin, Gustavo Deco, Peng Xie, and Jianfeng Feng

ABSTRACT

BACKGROUND: Resting-state functional connectivity reflects correlations in the activity between brain areas, whereas effective connectivity between different brain areas measures directed influences of brain regions on each other. Using the latter approach, we compare effective connectivity results in patients with major depressive disorder (MDD) and control subjects.

METHODS: We used a new approach to the measurement of effective connectivity, in which each brain area has a simple dynamical model, and known anatomical connectivity is used to provide constraints. This helps the approach to measure the effective connectivity between the 94 brain areas parceled in the automated anatomical labeling (AAL2) atlas, using resting-state functional magnetic resonance imaging. Moreover, we show how the approach can be used to measure the differences in effective connectivity between different groups of individuals, using as an example effective connectivity in the healthy brain and in individuals with depression. The first brainwide resting-state effective-connectivity neuroimaging analysis of depression, with 350 healthy individuals and 336 patients with major depressive disorder, is described.

RESULTS: Key findings are that the medial orbitofrontal cortex, implicated in reward and subjective pleasure, has reduced effective connectivity from temporal lobe input areas in depression; that the lateral orbitofrontal cortex, implicated in nonreward, has increased activity (variance) in depression, with decreased effective connectivity to and from cortical areas contralateral to language-related areas; and that the hippocampus, implicated in memory, has increased activity (variance) in depression and increased effective connectivity from the temporal pole.

CONCLUSIONS: Measurements of effective connectivity made using the new method provide a new approach to causal mechanisms in the brain in depression.

Keywords: Depression, Effective connectivity, Functional connectivity, Medial temporal lobe, Orbitofrontal cortex, Precuneus, Resting-state functional neuroimaging

<https://doi.org/10.1016/j.bpsc.2017.10.004>

Resting-state functional connectivity (FC), which is measured with functional magnetic resonance imaging (fMRI) and which reflects correlations in the activity between brain areas, is widely used to help understand human brain function in health and disease (1,2). Here we go beyond FC to investigate effective connectivity (EC) between different brain areas to measure directed influences of human brain regions on one other. EC is conceptually very different from FC, for it measures the effect of one brain region on another in a particular direction. Therefore, it can in principle provide information more closely related to the causal processes that operate in brain function—that is, how one brain region influences another. In the context of disorders of brain function, the EC differences between patients and control subjects may provide evidence on which brain regions may have altered function, and then influence other brain regions, and thereby be important in understanding the disorder.

In this study, we utilize a new approach to the measurement of EC, in which each brain area has a simple dynamical model and

known anatomical connectivity is used to provide constraints (3). This helps the approach to measure the EC between the 94 brain areas parceled in the Automated Anatomical Labeling (AAL2) atlas (4) using resting-state fMRI. Moreover, we show how the approach can be used to measure the differences in EC between different groups of individuals, using as an example EC in the healthy brain and in brains of individuals with depression. To the best of our knowledge, this article presents the first brainwide resting-state effective-connectivity neuroimaging analysis of depression, with results from 350 healthy individuals and 336 patients with major depressive disorder (MDD).

MDD is ranked by the World Health Organization as the leading cause of years-of-life lived with disability (5–8). Major depressive episodes, found in both MDD and bipolar disorder, are pathological mood states characterized by persistently sad or depressed mood. Major depressive episodes are generally accompanied by 1) altered incentive and reward processing, evidenced by amotivation, apathy, and anhedonia; 2) impaired modulation of anxiety and worry, manifested by generalized,

social, and panic anxiety, and oversensitivity to negative feedback; 3) inflexibility of thought and behavior in association with changing reinforcement contingencies, apparent as ruminative thoughts of self-reproach, pessimism, and guilt, and inertia toward initiating goal-directed behavior; 4) altered integration of sensory and social information, as evidenced by mood-congruent processing biases; 5) impaired attention and memory, shown as performance deficits on tests of attention set-shifting and maintenance, and autobiographical and short-term memory; and 6) visceral disturbances, including altered weight, appetite, sleep, and endocrine and autonomic function (5,7).

Patients with depression show impairments in the coordinated activity of several brain regions considered to be important for several domains of mental functioning, such as emotional processing (amygdala, subgenual anterior cingulate, and pallidum) (9,10), self-referential processes (medial prefrontal cortex, precuneus, and posterior cingulate cortex) (10–12), cognitive functions such as memory (hippocampus, parahippocampal cortex) (13), visual processing (fusiform gyrus, lingual gyrus, and lateral temporal cortex) (14), and attention processing (dorsolateral prefrontal cortex, anterior cingulate cortex, thalamus, and insula) (15).

Research into the pathophysiology of depression has included the analysis of possible differences in the FC of different brain areas to elucidate some of the brain changes that may relate to depression. Resting-state fMRI provides a task-free approach that removes some performance-related confounds, and it provides a reliable measure of baseline brain activity and connectivity (16). A meta-analysis of previous investigations of resting-state FC in depression was based on seed-based studies, each with tens of participants, and the analysis described hypoconnectivity within a frontoparietal network and hyperconnectivity within the default mode network, a network believed to support internally oriented and self-referential thought (17). In comparison, a recent study by Cheng *et al.* (2) included almost as many participants as this meta-analysis, did not need to rely on a priori, seed-based analyses, and was able, given its voxel-based approach, to provide detailed information about the exact brain regions involved rather than brain systems identified, for example, as the default mode network or frontoparietal control systems. In that first investigation using a voxel-based unbiased brainwide association study approach on resting-state fMRI data in 421 patients with MDD compared with 488 controls (2), Cheng *et al.* found decreased FC between the medial orbitofrontal cortex (OFC) (which has functions related to reward) with medial temporal lobe memory-related areas including the perirhinal cortex Brodmann area (BA) 36 and entorhinal cortex BA 28. We also found that the lateral OFC BA 47/12 (which has functions related to nonreward and punishment) had increased FC with the precuneus, the angular gyrus, and the temporal visual cortex BA 21 (2).

In the present research, we go beyond the FC approach, which reflects the interregion correlations of the observed activity, to EC, which estimates causal and directed interactions between brain regions. In essence, our model-based approach infers two sets of parameters from FC: the local fluctuating activity for each region of interest (e.g., excitability, described by the diagonal parameters of the matrix Σ) and the matrix of EC weights between the regions of interest (the

existence of connections is determined beforehand from diffusion tensor imaging data). Our dynamic model combines these parameters to generate EC, taking network effects into account at the whole-brain level. This approach may be useful in understanding the changes underlying depression, as it is not clear whether causes are circumscribed to the activity of a few nodes or to connectivity within a subnetwork. The new method that we use (3,18) has advantages and limitations compared with dynamic causal modeling (19–21) and is described in the Supplement.

To help understand some of the implications of the new findings described here, we note that there is considerable evidence that the medial and middle OFC is involved in reward, and that the lateral OFC is involved in nonreward and punishment (2,8,22–24). The hypotheses being investigated were that EC might be different in patients with depression and that the identification of which ECs were different may be useful in understanding the neural bases of depression.

METHODS AND MATERIALS

A brief description is provided here, with full details in the Supplement.

Participants

There were 336 patients with a diagnosis of major depressive disorder and 350 control subjects. The patients were from Xinan (First Affiliated Hospital of Chongqing Medical School in Chongqing, China) and Taiwan (Veteran General Hospital, Taipei).

Image Acquisition and Preprocessing

Data for resting-state connectivity analysis were collected in 3T MRI scanners (Siemens Trio, Erlangen, Germany) in an 8-minute period in which the participants were awake in the scanner and not performing a task, using standard protocols described here.

Data preprocessing was performed using DPARSF (<http://restfmri.net>); careful volume censoring (“scrubbing”) movement correction was performed as reported by Power *et al.* (25) to ensure that head-motion artifacts were not driving observed effects; and any effects of head motion were regressed out using the head motion parameters procedure described by Friston *et al.* (26).

EC Measurement

We used a new method that provides efficient calculation of maximum-likelihood EC estimates for a large number of nodes (94) (3). The method uses transitions of fMRI measurements across successive repetition times (volumes) and takes into account known anatomical connections. The effective connectivity model captures and uses this information via the covariances with nonzero time shifts. Both the EC in the model and the local input variance in a parameter Σ are optimized such that the model best reproduces statistics of the observed fMRI signals. Full details of the method are provided in the Supplement.

Two-tailed, two-sample *t* tests were performed on the normalized EC estimates to identify significantly altered effective connectivity links in patients compared to control subjects within each imaging center that provided resting-state fMRI data. The effects of age, gender ratios, head motion, and

Effective Connectivity in Depression

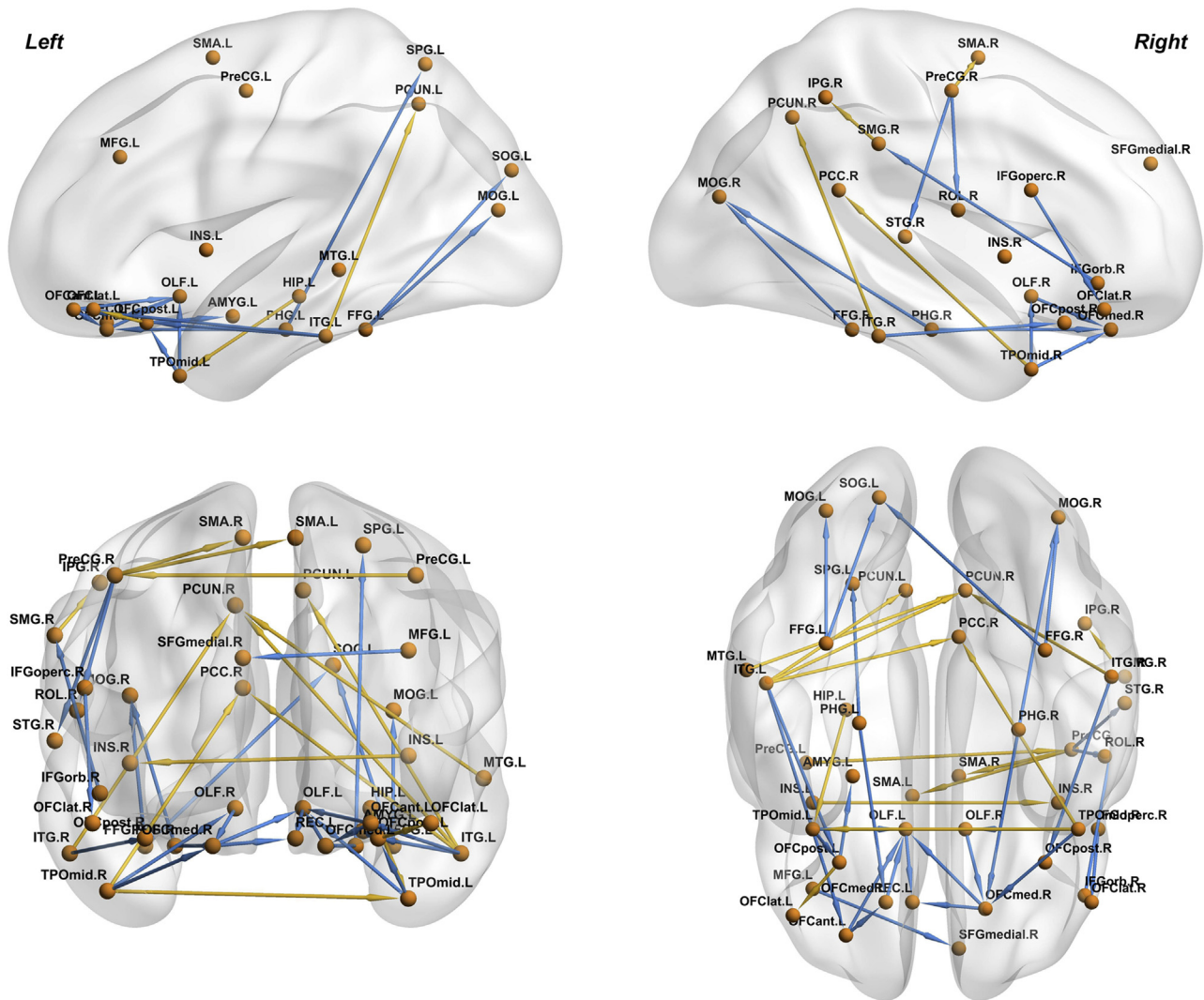


Figure 1. Differences in effective connectivity (EC) between patients with major depressive disorder and control subjects. The links shown are those with significantly different ECs after false discovery rate $p < .05$ correction. Yellow indicates that the EC is increased in patients compared with control subjects and blue that it is decreased. The direction of the stronger EC is indicated by an arrowhead in only one direction. If a link is decreased in strength in one direction in patients with depression, it is usually decreased in strength in the other direction, as shown in Table 1, and vice versa. If the ECs were similar (the ratio was < 1.5), then arrow heads are shown in both directions. The exact values and statistics for these links are provided in Table 1. Table 1 shows, for example, that although the forward connectivity from the visual areas classified as calcarine to the orbitofrontal cortex is increased in patients with major depressive disorder, the actual values for this EC are small. Only AAL2 regions are shown that have significantly different EC values in patients and control subjects on ≥ 1 side of the brain. The glass brains were generated using BrainNet Viewer (38).

education were regressed within each dataset in this step by general linear models. After obtaining the t test results for each center, the Liptak-Stouffer z score method was then used to combine the results from the individual datasets. Further, given that a reasonable effect size for effective connectivity is in the range 0.05 to 1 Hz for EC strengths, we consider here only EC differences greater than a threshold value of 0.01. Full details are provided in the Supplement.

RESULTS

The fMRI resting-state EC analyses were performed with 336 patients with a diagnosis of MDD and 350 control participants,

and this large population was sufficient to allow false discovery rate (FDR)-corrected statistics as described in detail elsewhere (2,27,28) with the 94 areas parceled in the AAL2 brain atlas (4) (see Supplemental Table S2 for the abbreviations for each area).

Differences in EC Between Patients With Depression and Controls

The results of the comparison of EC between patients with MDD and control subjects are shown in Figure 1 and Table 1. The results shown are those with significantly different EC links after FDR $p < .05$ correction, and with a

Table 1. Effective Connectivity Links Between Patients With Depression and Control Subjects

Region 1	Region 2	Region 1 AAL2 Name	Region 2 AAL2 Name	z Value for Forward ^{a,c}	p Value for Forward ^a	z Value for Backward ^c	p Value for Backward	EC of Forward in HC ^a	EC of Forward in MDD ^a	EC of Backward in HC	EC of Backward in MDD	EC Ratio in HC (Forward ^a / Backward)
Posterior orbital gyrus, left	Amygdala, left	OFCpost_L	Amygdala_L	-2.917	3.53E-03	-3.914	9.09E-05 ^b	0.012	0.009	0.009	0.007	1.345
Temporal pole: middle temporal gyrus, right	Posterior cingulate gyrus, right	Temporal_Pole_Mid_R	Cingulate_Post_R	2.225	2.61E-02	3.611	3.05E-04 ^b	0.021	0.022	0.003	0.003	7.433
Inferior temporal gyrus, left	Posterior cingulate gyrus, right	Temporal_Inf_L	Cingulate_Post_R	1.903	5.70E-02	3.557	3.75E-04 ^b	0.011	0.012	0.001	0.001	18.872
Middle frontal gyrus (area 2), left	Superior frontal gyrus, medial, right	Frontal_Mid_2_L	Frontal_Sup_Medial_R	-3.7	2.15E-04 ^b	-3.32	9.01E-04 ^b	0.011	0.008	0.004	0.003	2.635
Insula, left	Insula, right	Insula_L	Insula_R	0.193	8.47E-01	3.449	5.63E-04 ^b	0.028	0.028	0.018	0.018	1.534
Fusiform gyrus, left	Middle occipital gyrus, left	Fusiform_L	Occipital_Mid_L	-4.032	5.52E-05 ^b	0.31	7.56E-01	0.024	0.022	0.008	0.008	3.06
Fusiform gyrus, right	Middle occipital gyrus, right	Fusiform_R	Occipital_Mid_R	-3.717	2.02E-04 ^b	-1.211	2.26E-01	0.023	0.02	0.011	0.01	2.076
Parahippocampal gyrus, right	Middle occipital gyrus, right	ParaHippocampal_R	Occipital_Mid_R	-3.328	8.74E-04 ^b	-0.24	8.11E-01	0.016	0.013	0.007	0.006	2.386
Fusiform gyrus, right	Superior occipital gyrus, left	Fusiform_R	Occipital_Sup_L	-3.487	4.89E-04 ^b	-1.317	1.88E-01	0.023	0.02	0.005	0.005	4.167
Fusiform gyrus, left	Superior occipital gyrus, left	Fusiform_L	Occipital_Sup_L	-3.338	8.43E-04 ^b	-0.285	7.76E-01	0.024	0.021	0.005	0.005	4.77
Inferior temporal gyrus, left	Anterior orbital gyrus, left	Temporal_Inf_L	OFCant_L	-2.309	2.10E-02	-3.334	8.55E-04 ^b	0.014	0.012	0.006	0.005	2.225
Posterior orbital gyrus, left	Lateral orbital gyrus, left	OFCpost_L	OFClat_L	3.466	5.29E-04 ^b	-0.767	4.43E-01	0.018	0.02	0.008	0.008	2.238
Inferior frontal gyrus, opercular part, right	Lateral orbital gyrus, right	Frontal_Inf_Oper_R	OFClat_R	-1.462	1.44E-01	-3.74	1.84E-04 ^b	0.014	0.011	0.007	0.005	1.988
Parahippocampal gyrus, left	Medial orbital gyrus, left	ParaHippocampal_L	OFCmed_L	-3.247	1.17E-03 ^b	-1.209	2.27E-01	0.014	0.011	0.005	0.004	2.548
Anterior orbital gyrus, left	Medial orbital gyrus, left	OFCant_L	OFCmed_L	-3.168	1.54E-03 ^b	1.507	1.32E-01	0.019	0.016	0.015	0.015	1.224
Parahippocampal gyrus, right	Medial orbital gyrus, right	ParaHippocampal_R	OFCmed_R	-4.749	2.05E-06 ^b	-2.854	4.32E-03 ^b	0.013	0.01	0.005	0.003	2.815
Temporal pole: middle temporal gyrus, right	Medial orbital gyrus, right	Temporal_Pole_Mid_R	OFCmed_R	-5.084	3.70E-07 ^b	-4.014	5.98E-05 ^b	0.011	0.007	0.005	0.003	2.481
Olfactory cortex, right	Medial orbital gyrus, right	Olfactory_R	OFCmed_R	-3.255	1.14E-03 ^b	-2.897	3.76E-03	0.019	0.016	0.015	0.013	1.221
Temporal pole: middle temporal gyrus, left	Posterior orbital gyrus, left	Temporal_Pole_Mid_L	OFCpost_L	-3.443	5.76E-04 ^b	-3.051	2.28E-03	0.012	0.01	0.011	0.009	1.074

Table 1. Continued

Region 1	Region 2	Region 1 AAL2 Name	Region 2 AAL2 Name	z Value for Forward ^{a,c}	p Value for Forward ^a	z Value for Backward ^c	p Value for Backward	EC of Forward in HC ^a	EC of Forward in MDD ^a	EC of Backward in HC	EC of Backward in MDD	EC Ratio in HC (Forward ^a / Backward)
Inferior temporal gyrus, left	Posterior orbital gyrus, left	Temporal_Inf_L	OFCpost_L	-3.354	7.97E-04 ^b	-1.493	1.35E-01	0.013	0.01	0.006	0.005	2.081
Inferior temporal gyrus, right	Posterior orbital gyrus, right	Temporal_Inf_R	OFCpost_R	-2.765	5.70E-03	-3.383	7.18E-04 ^b	0.011	0.009	0.007	0.006	1.517
Medial orbital gyrus, right	Olfactory cortex, left	OFCmed_R	Olfactory_L	-2.716	6.61E-03	-3.535	4.07E-04 ^b	0.014	0.012	0.013	0.011	1.045
Medial orbital gyrus, left	Olfactory cortex, left	OFCmed_L	Olfactory_L	-2.697	7.00E-03	-3.41	6.49E-04 ^b	0.017	0.014	0.016	0.013	1.079
Temporal pole: middle temporal gyrus, left	Olfactory cortex, left	Temporal_Pole_Mid_L	Olfactory_L	-3.272	1.07E-03 ^b	-2.919	3.51E-03	0.01	0.008	0.006	0.004	1.814
Anterior orbital gyrus, left	Olfactory cortex, left	OFCant_L	Olfactory_L	-3.208	1.34E-03 ^b	-1.499	1.34E-01	0.011	0.009	0.007	0.006	1.622
Temporal pole: middle temporal gyrus, right	Olfactory cortex, right	Temporal_Pole_Mid_R	Olfactory_R	-3.761	1.69E-04 ^b	-3.283	1.03E-03 ^b	0.011	0.008	0.006	0.004	1.84
Supramarginal gyrus, right	Inferior parietal gyrus, excluding supramarginal gyrus and angular gyri, right	SupraMarginal_R	Parietal_Inf_R	0.706	4.80E-01	3.443	5.74E-04 ^b	0.023	0.022	0.013	0.014	1.741
Parahippocampal gyrus, left	Superior parietal gyrus, left	ParaHippocampal_L	Parietal_Sup_L	-3.983	6.81E-05 ^b	-1.636	1.02E-01	0.014	0.01	0.003	0.002	4.694
Precentral gyrus, left	Precentral gyrus, right	Precentral_L	Precentral_R	-2.222	2.63E-02	3.32	9.01E-04 ^b	0.021	0.018	0.02	0.021	1.032
Inferior temporal gyrus, left	Precuneus, left	Temporal_Inf_L	Precuneus_L	1.735	8.28E-02	3.179	1.48E-03 ^b	0.02	0.02	0.001	0.001	23.087
Inferior temporal gyrus, left	Precuneus, right	Temporal_Inf_L	Precuneus_R	2.879	3.99E-03	3.917	8.97E-05 ^b	0.014	0.015	0	0.001	31.401
Middle temporal gyrus, left	Precuneus, right	Temporal_Mid_L	Precuneus_R	2.915	3.56E-03	3.258	1.12E-03 ^b	0.011	0.012	0.001	0.001	12.235
Inferior temporal gyrus, right	Precuneus, right	Temporal_Inf_R	Precuneus_R	1.524	1.28E-01	3.215	1.31E-03 ^b	0.015	0.015	0.001	0.001	16.205
Olfactory cortex, left	Gyrus rectus, left	Olfactory_L	Rectus_L	-1.421	1.55E-01	-3.443	5.74E-04 ^b	0.017	0.016	0.012	0.01	1.42
Medial orbital gyrus, right	Gyrus rectus, left	OFCmed_R	Rectus_L	-0.657	5.11E-01	-3.237	1.21E-03 ^b	0.015	0.013	0.01	0.007	1.503
Precentral gyrus, right	Rolandic operculum, right	Precentral_R	Rolandic_Oper_R	-0.551	5.82E-01	-3.552	3.82E-04 ^b	0.02	0.02	0.015	0.012	1.347
Precentral gyrus, right	Supplementary motor area, left	Precentral_R	Supp_Motor_Area_L	3.786	1.53E-04 ^b	-0.046	9.63E-01	0.019	0.02	0.009	0.008	2.167
Precentral gyrus, right	Supplementary motor area, right	Precentral_R	Supp_Motor_Area_R	3.205	1.35E-03 ^b	-0.924	3.55E-01	0.019	0.02	0.013	0.012	1.412

Table 1. Continued

Region 1	Region 2	Region 1 AAL2 Name	Region 2 AAL2 Name	z Value for Forward ^{a,c}	z Value for Backward ^b	ρ Value for Forward ^{a,c}	ρ Value for Backward ^b	EC of Forward in HC ^a	EC of Backward in HC	EC of Forward in MDD ^a	EC of Backward in MDD	EC Ratio in HC (Forward/Backward)
Inferior frontal gyrus, pars orbitalis (area 2), right	Supramarginal gyrus, right	Frontal_Inf_Orb_2_R	SupraMarginal_R	-2.88	3.98E-03	-4.056	5.00E-05 ^b	0.015	0.012	0.01	0.008	1.507
Temporal pole: middle temporal gyrus, right	Temporal pole: middle temporal gyrus, left	Temporal_Pole_Mid_R	Temporal_Pole_Mid_L	0.509	6.11E-01	3.3	9.67E-04 ^b	0.026	0.025	0.019	0.02	1.376
Hippocampus, left	Temporal pole: middle temporal gyrus, left	Hippocampus_L	Temporal_Pole_Mid_L	1.611	1.07E-01	3.267	1.09E-03 ^b	0.012	0.013	0.007	0.008	1.625
Precentral gyrus, right	Superior temporal gyrus, right	Precentral_R	Temporal_Sup_R	-0.437	6.62E-01	-4.033	5.51E-05 ^b	0.017	0.016	0.009	0.007	1.787

Links are shown if their EC value in either direction exceeds the threshold of 0.01 and if there is a significant difference in at least one direction using false discovery rate correction for multiple comparisons, for which the significance level must be $p < .016$.

EC, effective connectivity; HC, healthy control group; L, left hemisphere; MDD, major depressive disorder group; R, right hemisphere.

^a“Forward” refers to the direction in which the link is strongest, in the direction from AAL2 region 1 to region 2.

^bThese values represent significant differences.

^cA negative value for z indicates a weaker EC link in patients with depression.

threshold for the $EC \geq 0.01$ healthy control subjects, patients with depression, or both. (This threshold on effect size precludes reporting trivial effects.) In Table 1, the forward direction is the direction with the higher EC (see the Supplement for further explanation). In Table 1, the results are grouped usefully according to the target region of the altered EC. We use this grouping by target brain regions to help describe the results for the main groups of differences of EC between patients and control subjects. The matrices of EC are shown in Supplemental Figure S1 for reference. We focus the discussion below on figures of the brain and tables showing the differences in EC, but Supplemental Figure S1 shows, for example, that temporal lobe areas 85–94 in AAL2 (Supplemental Table S2) tend to have high EC directed to the orbitofrontal areas (25–32) in healthy control subjects. Another interesting effect is that the FCs from frontal areas, including the inferior frontal gyrus (3–12) and lateral OFC (31, 32), are strong in the direction to supramarginal and angular gyri (65–70). Thus, EC provides useful information, emphasizing that medial OFC areas receive from the temporal cortex and that the lateral OFC/inferior frontal gyrus has strong forward connections to language areas. We emphasize that for most links that are different in patients with depression, the differences are in both the forward and backward ECs (see Table 1 and Supplemental Figure S2, FDR-corrected $p < .05$). What is new about the findings presented here is the direction of the forward versus the backward connectivity of these links that are different in depression, and this is emphasized in Figure 1 by larger arrowheads in the direction of the forward connectivity, defined as the direction with the greater EC.

Below we summarize some of the main points evident by inspection of Figure 1 and then provide a more detailed analysis, referring also to Table 1. One feature apparent in Figure 1 is that in depression, a number of areas including the parahippocampal gyrus, inferior temporal gyrus, and temporal pole have decreased EC directed to the medial and middle OFC areas. Another feature is that the fusiform gyrus has decreased EC directed to earlier visual cortical areas (occipital).

Medial and Middle OFC

The AAL2 regions included in this group and shown in Table 1 are the medial orbital gyrus, anterior orbital gyrus (OFCant), posterior orbital gyrus (OFCpost), rectus, and olfactory tubercle region at the posterior end of the OFC. This medial and middle OFC region has decreased EC (shown by a negative value for z in Table 1 and a blue arrow in Figure 1 into the target) from brain regions including the parahippocampal gyrus, temporal pole, inferior temporal gyrus, and amygdala. This implies less strong positive driving influences of these regions on the medial and middle OFC (see Table 1). Many of these ECs were much greater in the forward direction into the medial OFC than in the backward direction (Table 1). Both the forward and the backward ECs were in general lower in the group with depression than in the control subjects (Table 1).

There is also reduced EC between some of these different AAL2 regions in the medial and middle OFC (see Table 1).

Lateral OFC

The AAL2 regions included in this group and shown in Table 1 are the lateral orbital gyrus (OFClat) and inferior frontal gyrus, pars orbitalis (Frontal_Inf_Orb). The OFCpost (one of the middle OFC areas) has increased EC directed to the OFClat. Given that the medial OFC (which includes OFCpost) tends to be activated by rewards and the lateral OFC by nonrewards and punishers (23,29) and given that they are reciprocally activated by reward and loss (30), we sought to elucidate the interpretation of this increase in EC from medial to lateral OFC in depression. The EC measure does not specify whether this should be interpreted as increased excitatory input from the medial to the lateral OFC or as an increased connectivity that might reflect that any change in medial OFC produces a larger change, but in the opposite (reciprocal) direction. We reasoned that the FC between the medial and lateral OFC might provide relevant evidence. What we found, in summary, is that all the medial OFC areas (medial orbital gyrus, OFCant, OFCpost, rectus, and posterior end of the OFC) have a high FC with one another that is on average 0.58 (SD 0.13) (in the control group). Similarly, the two lateral OFC areas (OFClat and inferior frontal gyrus, pars orbitalis [IFG_Orb]) have high FC with each other that is on average 0.68 (SD 0.08). However, the mean FC between the medial OFC areas and lateral OFC areas was much lower, 0.36 (SD 0.16), and the difference was significant (t test, $p < 10^{-12}$). Further, this relates to an average FC value across all pairs in the brain of 0.35. This evidence indicates that the medial and lateral OFC areas are not positively coupled to

each other but can operate in opposite directions and even could operate reciprocally. We thus interpret the increased EC from medial to lateral OFC as consistent with the hypothesis that underactivity in the medial OFC in depression (2,8) may be one of the reasons that lateral OFC activity is high in depression, for which evidence is described below and elsewhere (2,8).

In addition, the inferior frontal gyrus opercular part back connection to the lateral OFC is reduced in depression. The supramarginal gyrus has decreased EC with the inferior frontal gyrus, pars orbitalis (Frontal_Inf_Orb_2) in depression. The right supramarginal gyrus also has decreased EC in both directions with right OFClat.

Temporal Lobe

The temporal lobe areas with different ECs in depression include the temporal pole and the inferior and middle temporal gyrus. Most of these areas have reduced forward EC directed to medial and middle OFC areas including medial orbital gyrus and OFCant. (Although Table 1 shows significant increases in the back projection to the temporal areas from the precuneus, we discount these because these back-projection ECs are so very low.)

Hippocampus and Parahippocampal Gyrus

The EC directed from the temporal pole to the hippocampus is increased in depression. As noted above, the EC from the

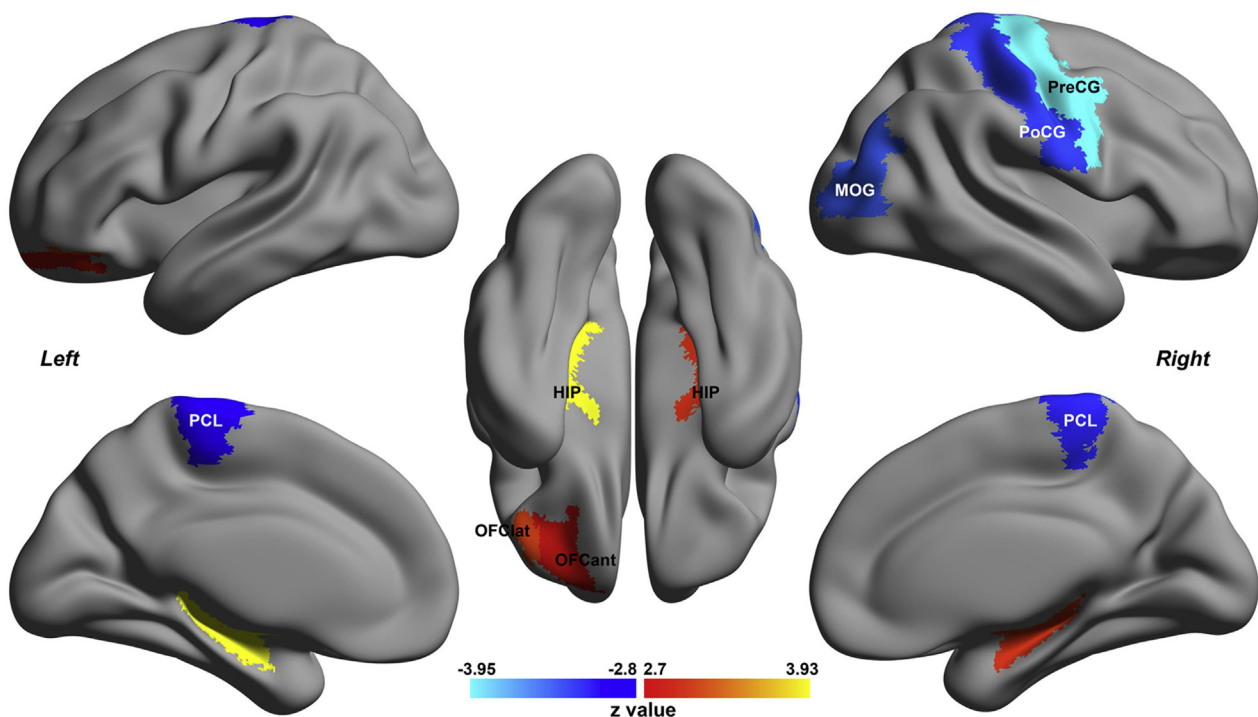


Figure 2. The results of the comparison of Σ between patients with major depressive disorder and healthy control subjects. This figure shows the significant AAL2 areas after false discovery rate $p < .05$ correction. Normalization of Σ was used, applied in the same way as for the effective connectivity. Red-yellow indicates AAL2 regions with increased Σ , and blue those with decreased Σ (see Table 2). HIP, hippocampus; MOG, middle occipital gyrus; OFCant, anterior orbital gyrus; OFClat, lateral orbital gyrus; PCL, paracentral lobule; PoCG, postcentral gyrus; PreCG, precentral gyrus.

Table 2. Σ Values for AAL2 Regions Significantly Different (False Discovery Rate–Corrected) Between Patients With Depression and Control Subjects

Region	Region AAL2 Name	z Value of Σ	p Value of Σ	Σ of HC ^a	Σ of MDD
Precentral gyrus, right	Precentral_R	−3.946	7.96E−05	−0.288	−0.481
Hippocampus, left	Hippocampus_L	3.926	8.64E−05	−0.942	−0.891
Middle occipital gyrus, right	Occipital_Mid_R	−3.295	9.83E−04	−0.309	−0.378
Lenticular nucleus, putamen, left	Putamen_L	3.212	1.32E−03	−0.896	−0.854
Postcentral gyrus, right	Postcentral_R	−3.154	1.61E−03	−0.258	−0.400
Lateral orbital gyrus, left	OFClat_L	3.068	2.16E−03	1.086	1.253
Paracentral lobule, right	Paracentral_Lobule_R	−3.058	2.23E−03	1.001	0.647
Hippocampus, right	Hippocampus_R	2.980	2.88E−03	−0.989	−0.942
Paracentral lobule, left	Paracentral_Lobule_L	−2.936	3.33E−03	0.776	0.461
Anterior orbital gyrus, left	OFCant_L	2.777	5.48E−03	−0.464	−0.356

HC, healthy control group; left, left hemisphere; MDD, major depressive disorder group; right, right hemisphere.

^aThe Σ of HC shown is the mean after normalization within each participant.

parahippocampal gyrus to the medial OFC areas (and to the superior parietal lobule) is decreased in depression.

Precuneus

Four forward links from the left inferior/middle temporal gyrus to the precuneus have increased EC in depression (Table 1 and Figure 1). It is notable that these links have a much greater strength in the forward than in the backward direction, with a mean ratio of >20 (Table 1). (It is noted that separately each of these forward links did not quite reach the threshold required for FDR correction, although the strengths in the backward direction did.)

Sensorimotor Cortical Areas

The precentral gyrus (motor cortex) has increased EC directed to some other motor areas, including the supplementary motor area.

Differences in Both Forward and Backward EC in Depression

The results of the comparison of EC (forward vs. backward) between MDD and healthy control subjects are shown in Supplemental Figure S2. The main implication of this figure is that links change similarly in both directions in depression. That is, if an EC link is stronger in one direction in depression, it is likely to be stronger in the other direction, too; and if a link is weaker in one direction in depression, it is likely to be weaker in the opposite direction, too ($r = .44$, $p < .0001$).

Differences in Σ , the Spontaneous Activity Parameter, Between Patients With MDD and Control Subjects

The results of the comparison of the spontaneous activity parameter Σ between MDD and healthy control subjects are shown in Figure 2 and Table 2. Σ values for AAL2 regions significantly different (FDR-corrected $p < .05$) between patients with depression and control subjects are shown.

One point of interest is that Σ for the right and left hippocampus is significantly increased in patients with MDD. This is in the context that the EC directed from the temporal pole to the hippocampus is increased in depression.

A second point of interest is that Σ for the lateral OFC (OFClat_L) is significantly increased in patients with MDD. This effect spread as far medially as at least a part of OFCant_L. For comparison, the value of Σ for OFClat_R was also increased in MDD ($p < .05$, uncorrected).

These findings are consistent with the hypothesis that in MDD there is increased activity in the lateral OFC (a region involved in nonreward and punishment) and the hippocampus (a region involved in memory) (2,8).

Correlations Between the EC Links and the MDD Severity

Correlations between the EC links and the MDD symptom severity scores, in particular, the illness duration, are shown in Supplemental Table S3. These results indicate that the differences in EC that were found are related to the severity of the MDD. Further evidence consistent with this is that some of the EC links were correlated with the scores on the Beck Depression Inventory, the Hamilton Depression Rating Scale, and the Hamilton Anxiety Rating Scale, as shown in Supplemental Table S3. (This information is provided to help interpret the findings; we do not rely on these correlations, because they are not corrected for multiple comparisons.)

Summary Diagram

A summary of the networks that show different EC in patients with MDD is shown in Figure 3. A decrease in EC is shown in blue and an increase in red.

DISCUSSION

In this investigation of EC with 336 patients with MDD and 350 controls, the key findings are that the medial OFC, implicated in reward and subjective pleasure, has reduced EC from temporal lobe areas in depression; that the lateral OFC, implicated in nonreward, has increased activity in depression, with decreased EC to and from areas contralateral to language-related areas (including supramarginal gyrus); and that the hippocampus, implicated in memory, has increased activity in depression and increased EC from the temporal pole.

Effective Connectivity in Depression

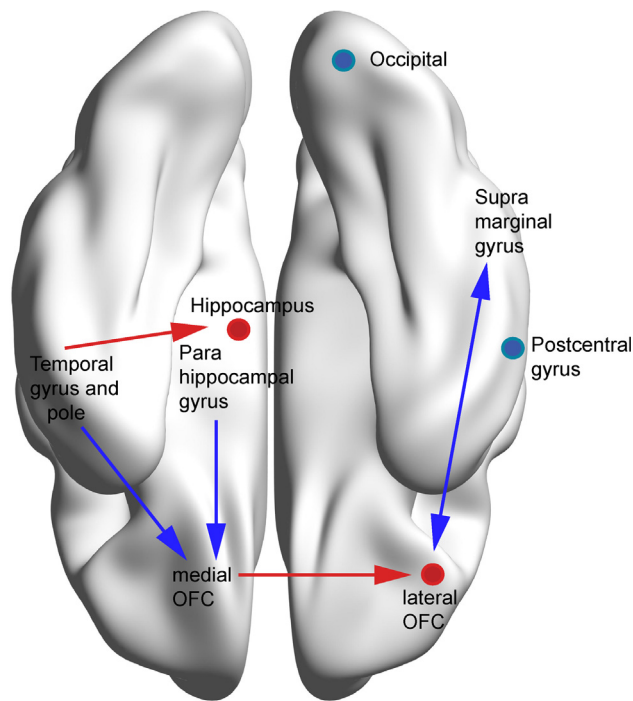


Figure 3. Summary of the networks that show different effective connectivity in patients with depression, shown on a ventral view of the brain. A decrease in effective connectivity in patients with major depressive disorder is shown in blue, and an increase in red. In most cases there was a similar change in the effective connectivity in both directions in depression. The direction of the arrows shows though the direction of the stronger (termed forward) effective connectivity. Regions with an increased value of Σ , reflecting increased activity, are indicated by a red circle; regions with a decreased value of Σ are indicated by a blue circle. For further details of the differences in the effective connectivities and the side of the brain on which they are present, see [Table 1](#) and [Figure 1](#). OFC, orbitofrontal cortex.

We found that EC directed to the medial OFC from areas including the parahippocampal gyrus, temporal pole, inferior temporal gyrus, and amygdala were decreased in MDD. This is the forward direction for most of these links. This implies less strong positive driving influences of these input regions on the medial and middle OFC, regions implicated in reward, and thus helps to elucidate part of the decreased feelings of happy states in depression (8). The forward links from temporal cortical areas to the precuneus are increased in depression (and are close to significant after FDR correction), and this may relate to representations of the sense of self (31), which become more negative in depression (2,8). The lateral OFC areas have reduced EC with the (mainly right) inferior frontal gyrus opercular part and directed to the supramarginal gyrus. In addition, the lateral OFC, an area implicated in nonreward and punishment, had an increased level of activity as reflected in Σ in the MDD group. A notable finding was that Σ was also increased in the right and left hippocampus of patients with depression, suggesting some type of heightened memory-related processing in the context that the EC directed from the temporal pole to the hippocampus is increased in depression. Together these differences are consistent with the hypothesis that some aspects of

hippocampal processing, perhaps those related to unpleasant memories, are increased in depression (2,8) and that the influence of temporal lobe memory systems on specifically the medial OFC is reduced in depression. The value of EC in understanding the operation of these systems in depression is that although the FC (which reflects correlations) between these areas has been shown to be reduced in depression (2), it is only by using EC that we understand better the direction of the major influence between these brain regions (from the temporal lobe to the medial OFC), and, for example, that this directed connectivity is reduced in depression ([Figure 3](#) and [Table 1](#)).

The findings for different brain systems are now considered, putting together the results not only of the EC analysis described here, but also of the large analysis of FC in patients with depression (2).

An interesting finding of the investigation is that the medial (which include the middle) OFC-related areas receive forward projections from the temporal cortex areas as shown by the EC measure. This is consistent with macaque neuroanatomy (32,33) and with the fact that these medial OFC areas have responses to visual, taste, olfactory, somatosensory, and auditory inputs, which must originate from temporal, insular, olfactory, etc., areas. The medial OFC areas have neuronal responses in macaques and fMRI activations in humans, which show that they represent the reward value of these stimuli (22,23,29,34). The implication is that the reduced forward inputs into the medial OFC in depression relate to the decrease in positively affective states that are present in depression and that this is one of the key brain changes related to depression (2,8,35–37). This hypothesis is supported by the finding that the decrease in the EC to the anterior OFC from temporal lobe areas is correlated with the severity of the depression as assessed by the duration of the illness ([Supplemental Table S3](#)).

With respect to the lateral OFC, we previously reported that there is increased FC between the lateral OFC and the precuneus, angular gyrus, and inferior temporal cortex (2). In the context of the functions of the lateral OFC in nonreward and punishment (8,24), this increased FC was related to increased negative value of the self (low self-esteem) (precuneus), to increased language-based negative thoughts (rumination) (angular gyrus), and to increased aversive or nonrewarding effects of some visual stimuli (inferior temporal cortex) (2). The new findings presented here provide supporting complementary evidence. For example, the activity as reflected by Σ was increased in the lateral OFC of patients with MDD ([Table 2](#)), consistent with increased nonreward and/or aversive processing in depression being implemented by the lateral OFC (8,24). The right inferior frontal gyrus opercular part (BA 44) connection from the lateral OFC is reduced in depression. The inferior frontal gyrus, pars orbitalis (a lateral part of the lateral OFC) has reduced EC from the right supramarginal gyrus. Thus, the lateral OFC has a number of reduced ECs with areas mainly contralateral to language-related areas. The most interesting finding was the increase in activity (assessed by Σ) in the lateral OFC in depression, which, taken with the increased FC with the precuneus and language areas in depression (2), supports the hypothesis that low self-esteem and high rumination are related to the connections to these two areas in depression.

The link from the inferior temporal gyrus and temporal pole to the right posterior cingulate cortex is increased in depression. These complementary findings serve to draw attention to the altered functioning of the precuneus (and connected posterior cingulate cortex), which is involved in representations of the self (31), in depression. The relevant circuit may include the lateral OFC, precuneus, posterior cingulate, and temporal lobe cortical areas.

Although it was not a primary aim of this investigation, the effects of medication were assessed by comparing the FC in 125 patients not receiving medication and 157 patients receiving medication. The overall pattern of FC differences between patients and controls is similar for the unmedicated and the medicated subgroups of patients (Supplemental Figure S4), providing evidence that the main differences between patients and control subjects shown in Figure 1 were found in patients with depression whether or not they were receiving medication. Further details are provided in the Supplement.

In this large-scale test of the EC algorithm (3), we show that it has potential to elucidate processing in the brain that goes beyond correlations between brain areas (FC) to directed connectivity between brain areas (EC). The approach thus provides evidence on how one brain area may influence another. Part of the power of the approach compared with other approaches is that evidence on the anatomical connectivity of the brain is taken into account. The research described here thus makes a contribution to understanding brain structure and function, and indeed how structure and function are related in both normal and disordered brain function.

ACKNOWLEDGMENTS AND DISCLOSURES

JF is a Royal Society Wolfson Research Merit Award holder. JF is also partially supported by the National High Technology Research and Development Program of China (Grant No. 2015AA020507) and the key project of Shanghai Science & Technology Innovation Plan (Grant No. 15JC1400101). The research was partially supported by the National Centre for Mathematics and Interdisciplinary Sciences (NCMIS) of the Chinese Academy of Sciences, Key Program of National Natural Science Foundation of China (Grant No. 91230201), and the Shanghai Soft Science Research Program (Grant No. 15692106604). WC is supported by grants from the National Natural Sciences Foundation of China (Grant No. 81701773, 11771010, 11471081, 11101429, and 71661167002), sponsored by Shanghai Sailing Program (Grant No. 17YF1426200) and the Research Fund for the Doctoral Program of Higher Education of China (Grant No. 2017M610226). C-PL was supported in part by funding from Ministry of Science and Technology, Taiwan (Grant Nos. NSC100-2911-I-010-010-010, NSC101-2911-I-010-009, NSC100-2628-E-010-002-MY3, NSC102-2321-B-010-023, and NSC103-2911-I-010-501), National Health Research Institutes (Grant Nos. NHRI-EX103-10310E and NHRI-EX106-10611E), Ministry of Health and Welfare of Taiwan (Grant No. DOH102-TD-PB-111-NSC006), and Academia Sinica, Taipei, Taiwan. JQ was supported by the National Natural Science Foundation of China (Grant Nos. 31271087, 31470981, 31571137, 31500885), National Outstanding Young People Plan, the Program for the Top Young Talents by Chongqing, the Fundamental Research Funds for the Central Universities (Grant No. SWU1509383), Natural Science Foundation of Chongqing (Grant No. cstc2015jcyjA10106), and a general financial grant from the China Postdoctoral Science Foundation (Grant No. 2015M572423). PX is supported by the National Science Foundation of China (Grant No. NSFC 31271189). The effective connectivity algorithm work was supported by the Human Brain Project (Grant No. FP7-FET-ICT-604102 and H2020-720270 HBP SGA1 to GD) and the Marie Skłodowska-Curie Action (Grant No. H2020-MSCA-656547 to MG).

ETR, MG, WC, and JF contributed to the design of the study. JQ, ZH, HR, YL, C-CH, ACY, S-JT, XZ, KZ, C-PL, and PX contributed to the collection of the data. WC, ETR, and MG contributed to the analysis of the data and the preparation of the manuscript. ETR, WC, and MG participated in writing the paper, with GD in the interpretation of the findings. All collaborators had an opportunity to contribute to the interpretation of the results and to the drafting of the manuscript.

The authors report no biomedical financial interests or potential conflicts of interest.

ARTICLE INFORMATION

From the Department of Computer Science (ETR, WC, JF), University of Warwick, Coventry, United Kingdom; Oxford Centre for Computational Neuroscience (ETR), Oxford, United Kingdom; Institute of Science and Technology for Brain-Inspired Intelligence (WC, HR, C-PL, JF), School of Mathematical Sciences (HR, JF), and School of Life Science and the Collaborative Innovation Center for Brain Science (JF), Fudan University, Shanghai, PR China; Center for Brain and Cognition, Computational Neuroscience Group, Department of Information and Communication Technologies (MG, GD), and Institutió Catalana de la Recerca i Estudis Avançats (GD), Universitat Pompeu Fabra, Barcelona, Spain; Key Laboratory of Cognition and Personality, Southwest University, Ministry of Education (JQ), Department of Psychology, Southwest University (JQ, YL, KZ), Institute of Neuroscience, Chongqing Medical University (ZH, XZ, PX), Chongqing Key Laboratory of Neurobiology (ZH, XZ, PX), and Department of Neurology, The First Affiliated Hospital of Chongqing Medical University (ZH, XZ, PX), Chongqing, China; and Institute of Neuroscience, National Yang-Ming University (CCH, C-PL), Department of Psychiatry, Taipei Veterans General Hospital (ACY, S-JT), and Brain Research Center, National Yang-Ming University (C-PL), Taipei, Taiwan.

ETR, WC, MG, JQ, and ZH contributed equally to this work.

Address correspondence to Edmund T. Rolls, D.Sc., University of Warwick, Computer Science, Coventry CV47AL, UK; E-mail: Edmund.Rolls@oxcns.org; or Jianfeng Feng, Ph.D., Centre for Computational Systems Biology, School of Mathematical Sciences, Fudan University, Shanghai 200433, China, or Department of Computer Science, University of Warwick, Coventry CV4 7AL, UK; E-mail: jianfeng64@gmail.com; or Professor Peng Xie, Department of Neurology, The First Affiliated Hospital of Chongqing Medical University, Chongqing, 400016, PR China; E-mail: xiepeng@cqmu.edu.cn; or Professor Ching-Po Lin, Institute of Neuroscience, National Yang-Ming University, Taipei, Taiwan; E-mail: cplin@ym.edu.tw.

Received May 5, 2017; revised Oct 10, 2017; accepted Oct 11, 2017.

Supplementary material cited in this article is available online at <https://doi.org/10.1016/j.bpsc.2017.10.004>.

REFERENCES

- Deco G, Kringelbach ML (2014): Great expectations: Using whole-brain computational connectomics for understanding neuropsychiatric disorders. *Neuron* 84:892–905.
- Cheng W, Rolls ET, Qiu J, Liu W, Tang Y, Huang CC, *et al.* (2016): Medial reward and lateral non-reward orbitofrontal cortex circuits change in opposite directions in depression. *Brain* 139:3296–3309.
- Gilson M, Moreno-Bote R, Ponce-Alvarez A, Ritter P, Deco G (2016): Estimation of directed effective connectivity from fMRI functional connectivity hints at asymmetries in the cortical connectome. *PLoS Comput Biol* 12:e1004762.
- Rolls ET, Joliot M, Tzourio-Mazoyer N (2015): Implementation of a new parcellation of the orbitofrontal cortex in the automated anatomical labeling atlas. *Neuroimage* 122:1–5.
- Drevets WC (2007): Orbitofrontal cortex function and structure in depression. *Ann N Y Acad Sci* 1121:499–527.
- Hamilton JP, Chen MC, Gotlib IH (2013): Neural systems approaches to understanding major depressive disorder: an intrinsic functional organization perspective. *Neurobiol Dis* 52:4–11.
- Gotlib IH, Hammen CL (2009): *Handbook of Depression*. New York: Guilford Press.

Effective Connectivity in Depression

8. Rolls ET (2016): A non-reward attractor theory of depression. *Neurosci Biobehav Rev* 68:47–58.
9. Disner SG, Beevers CG, Haigh EA, Beck AT (2011): Neural mechanisms of the cognitive model of depression. *Nat Rev Neurosci* 12:467–477.
10. Sheline YI, Price JL, Yan Z, Mintun MA (2010): Resting-state functional MRI in depression unmasks increased connectivity between networks via the dorsal nexus. *Proc Natl Acad Sci U S A* 107:11020–11025.
11. Kuhn S, Gallinat J (2013): Resting-state brain activity in schizophrenia and major depression: a quantitative meta-analysis. *Schizophr Bull* 39:358–365.
12. Price JL, Drevets WC (2010): Neurocircuitry of mood disorders. *Neuropsychopharmacology* 35:192–216.
13. Lorenzetti V, Allen NB, Fornito A, Yucel M (2009): Structural brain abnormalities in major depressive disorder: a selective review of recent MRI studies. *J Affect Disord* 117:1–17.
14. Veer IM, Beckmann CF, van Tol MJ, Ferrarini L, Milles J, Veltman DJ, *et al.* (2010): Whole brain resting-state analysis reveals decreased functional connectivity in major depression. *Front Syst Neurosci* 4.
15. Hamilton JP, Etkin A, Furman DJ, Lemus MG, Johnson RF, Gotlib IH (2012): Functional neuroimaging of major depressive disorder: a meta-analysis and new integration of base line activation and neural response data. *Am J Psychiatry* 169:693–703.
16. Gusnard DA, Raichle ME, Raichle ME (2001): Searching for a baseline: functional imaging and the resting human brain. *Nat Rev Neurosci* 2:685–694.
17. Kaiser RH, Andrews-Hanna JR, Wager TD, Pizzagalli DA (2015): Large-scale network dysfunction in major depressive disorder: A meta-analysis of resting-state functional connectivity. *JAMA Psychiatry* 72:603–611.
18. Gilson M, Deco G, Friston KJ, Hagmann P, Mantini D, Betti V, *et al.* (2017): Effective connectivity inferred from fMRI transition dynamics during movie viewing points to a balanced reconfiguration of cortical interactions [published online ahead of print Oct 9]. *Neuroimage*.
19. Valdes-Sosa PA, Roebroeck A, Daunizeau J, Friston K (2011): Effective connectivity: influence, causality and biophysical modeling. *Neuroimage* 58:339–361.
20. Bajaj S, Adhikari BM, Friston KJ, Dhamala M (2016): Bridging the gap: Dynamic causal modeling and Granger causality analysis of resting state functional magnetic resonance imaging. *Brain Connect* 6:652–661.
21. Friston K (2009): Causal modelling and brain connectivity in functional magnetic resonance imaging. *PLoS Biol* 7:e33.
22. Rolls ET (2014): *Emotion and Decision-Making Explained*. Oxford: Oxford University Press.
23. Grabenhorst F, Rolls ET (2011): Value, pleasure, and choice in the ventral prefrontal cortex. *Trends Cogn Sci* 15:56–67.
24. Rolls ET (2017): The roles of the orbitofrontal cortex via the habenula in non-reward and depression, and in the responses of serotonin and dopamine neurons. *Neurosci Biobehav Rev* 75:331–334.
25. Power JD, Mitra A, Laumann TO, Snyder AZ, Schlaggar BL, Petersen SE (2014): Methods to detect, characterize, and remove motion artifact in resting state fMRI. *Neuroimage* 84:320–341.
26. Friston KJ, Williams S, Howard R, Frackowiak RS, Turner R (1996): Movement-related effects in fMRI time-series. *Magn Reson Med* 35:346–355.
27. Cheng W, Rolls ET, Gu H, Zhang J, Feng J (2015): Autism: Reduced functional connectivity between cortical areas involved in face expression, theory of mind, and the sense of self. *Brain* 138:1382–1393.
28. Cheng W, Palaniyappan L, Li M, Kendrick KM, Zhang J, Luo Q, *et al.* (2015): Voxel-based, brain-wide association study of aberrant functional connectivity in schizophrenia implicates thalamocortical circuitry. *NPJ Schizophr* 1:15016.
29. Rolls ET, Grabenhorst F (2008): The orbitofrontal cortex and beyond: From affect to decision-making. *Prog Neurobiol* 86:216–244.
30. O’Doherty J, Kringelbach ML, Rolls ET, Hornak J, Andrews C (2001): Abstract reward and punishment representations in the human orbitofrontal cortex. *Nat Neurosci* 4:95–102.
31. Cavanna AE, Trimble MR (2006): The precuneus: a review of its functional anatomy and behavioural correlates. *Brain* 129:564–583.
32. Pandya DN, Seltzer B, Petrides M, Cipolloni PB (2015): *Cerebral Cortex: Architecture, Connections, and the Dual Origin Concept*. New York: Oxford University Press.
33. Saleem KS, Kondo H, Price JL (2008): Complementary circuits connecting the orbital and medial prefrontal networks with the temporal, insular, and opercular cortex in the macaque monkey. *J Comp Neurol* 506:659–693.
34. Rolls ET (2017): The orbitofrontal cortex and emotion in health and disease, including depression [published online ahead of print Sep 24]. *Neuropsychologia*.
35. Eshel N, Roiser JP (2010): Reward and punishment processing in depression. *Biol Psychiatry* 68:118–124.
36. Nusslock R, Young CB, Damme KS (2014): Elevated reward-related neural activation as a unique biological marker of bipolar disorder: Assessment and treatment implications. *Behav Res Ther* 62:74–87.
37. Price JL, Drevets WC (2012): Neural circuits underlying the pathophysiology of mood disorders. *Trends Cogn Sci* 16:61–71.
38. Xia M, Wang J, He Y (2013): BrainNet Viewer: A network visualization tool for human brain connectomics. *PLoS One* 8:e68910.